

## Numerical simulation of soil-structure interaction in framed and shear-wall structures

M. Dalili<sup>1,2</sup>, A. Alkarni<sup>3</sup>, J. Noorzai<sup>\*1,2</sup>, M. Paknahad<sup>1,2</sup>, M.S. Jaafar<sup>1</sup> and B.B.K. Huat<sup>1</sup>

<sup>1</sup>*Civil Engineering Faculty, Universiti Putra Malaysia, Malaysia*

<sup>2</sup>*Institute of Advanced Technology, Universiti Putra Malaysia, Malaysia*

<sup>3</sup>*Civil Engineering Faculty, King Saud University, Riyadh, Saudi Arabia*

*(Received September 13, 2010, Accepted January 26, 2011)*

**Abstract.** This paper deals with the modeling of the plane frame structure-foundation-soil system. The superstructure along with the foundation beam is idealized as beam bending elements. The soil medium near the foundation beam with stress concentrated is idealized by isoparametric finite elements, and infinite elements are used to represent the far field of the soil media. This paper presents the modeling of shear wall structure-foundation and soil system using the optimal membrane triangular, super and conventional finite elements. Particularly, an alternative formulation is presented for the optimal triangular elements aimed at reducing the programming effort and computational cost. The proposed model is applied to a plane frame-combined footing-soil system. It is shown that the total settlement obtained from the non-linear interactive analysis is about 1.3 to 1.4 times that of the non-interactive analysis. Furthermore, the proposed model was found to be efficient in simulating the shear wall-foundation-soil system, being able to yield results that are similar to those obtained by the conventional finite element method.

**Keywords:** triangular element; shear wall structure; super element; drilling degree of freedom.

---

### 1. Introduction

The interaction among structures, their foundations and the soil medium below the foundations considerably alters the behavior of the structure compared with the case where the structure is considered alone. Thus, a reasonably accurate model for the soil-foundation-structure interaction system with computational validity and efficiency is needed to improve the design of important structures.

Extensive research was conducted by Viladkar and co-workers on 2D and 3D framed structure-foundation-soil interaction problems, as well as shear wall foundation-soil systems (Viladkar, Godbole *et al.* 1991, Viladkar, Godbole *et al.* 1992, Viladkar, Godbole *et al.* 1994, Viladkar, Noorzai *et al.* 1994, Viladkar, Sharma *et al.* 1992). They employed the isoparametric beam bending element to represent the superstructure and the coupled finite and infinite elements to model the near and far fields of soil media, respectively. The superstructure materials were assumed to obey the Hookean law, while the stress-strain relationships of the soil were considered as nonlinear elastic. In the study by (Pandey, Kumar *et al.* 1994), an iterative approach was proposed for the soil-structure interaction

---

\* Corresponding author, Ph.D., E-mail: [jamal@eng.upm.edu.my](mailto:jamal@eng.upm.edu.my)

of tall buildings having closely spaced independent footings. In order to verify the proposed approach, a finite element analysis was carried out for a 10 storey plane frame. The computational effort was shown to be less than that needed for the conventional finite element analysis.

A comprehensive review on the modeling of soil-structure-foundation system was presented in Dutta and Roy (2002), in which an attempt was made to review the possible models available in the literature for soil structure interaction analysis. Major attention was focused on the physical modeling of the soil media. The authors concluded that the Winkler theory, despite its obvious limitations, yields reasonable performance and it is easy to exercise. Therefore, for practical purpose, such an idealization should be employed, instead of using structures with fixed base. Furthermore, the effect of material nonlinearity, non-homogeneity and anisotropy of the supporting soil medium should be taken into account.

The method presented by Fan *et al.* (2005), applicable for the analysis of superstructure-foundation interaction, was a method combining the analytical solution with finite element method. This method enables us to obtain the nodal forces of the superstructure and pile-soil system, bending and torsional moments, and the normal and shear stresses at any point in the raft foundation.

A new method was proposed by Badie and co-workers for analyzing shear wall structures on elastic foundations. The soil is modeled using a three-nodded quadratic element that includes the vertical sub grade reaction technique and soil shear stiffness (Badie and Salmon 1996, 1997, Badie, Salmon *et al.* 1997). In their studies, two types of soil were assumed, namely, dense sand and soft clay, and the flexibility for the base of shear walls was modeled by the Winkler model. It was observed that the maximum drift is about six times that of a rigid foundation for dense sand and about three hundred times that of a rigid foundation for soft clay.

Nadjai and Johnson (1998) investigated the importance of base flexibility on the behavior of planar shear walls subjected to lateral loading. A simple analytical model with basic assumptions was proposed and compared the results obtained with the recorded response (Boroschek and Yáñez 2000). Super element was presented for the analysis of shear walls with opening (Kim and Lee 2003).

Soil-pile-structure interaction of a two bay single storey frame was carried out considering a group pile embedded in clayey soil supporting a flexible cap to study the effect of pile cap-soil interaction and piles configuration and spacing on the maximum displacement at the top of the frame and on the moments in columns of the superstructure (Chore *et al.* 2009). Influence of soil-pile interaction has been found considerable on the behavior of pile cap-soil media.

The above study has been further extended by Chore *et al.* (2010a, b) where authors introduced a modified finite element idealization through idealizing the soil, pile and pile cap with linear spring element, one dimensional twenty-nodded iso-parametric continuum beam element and two dimensional twenty-nodded iso-parametric continuum plate element respectively. The three major focus points considered in their uncoupled analysis have been pile spacing, configuration of the piles and diameter of the piles on the behavior of the superstructure.

Two group piles were considered one including two piles and another one with three piles. With the proposed idealization method the effect of interaction was found to be significant with a considerable amount of superstructure displacement compared to the fixed based structure.

It is clear from the above literature review that so far no attempt has been made to consider: (a) numerical simulation of framed structures pile foundation-soil on the slope, (b) numerical model that includes the super element or drilling element and conventional finite elements for simulation of the shear wall foundation and soil media as a single compatible unit. The present study is a continuation of authors' previous works (Noorzaei, Alkarni *et al.* 2010, Paknahad, Noorzaei *et al.* 2007, Paknahad, Noorzaei *et al.* 2009), who analyzed a shear wall structure using the optimal

membrane triangular element. Hence the objective of this study is focused on:

- (i) Modelling of framed structures-pile foundation – soil media built on inclined strata.
- (ii) Modelling of shear wall-foundation using modified optimum triangular element with drilling degree of freedom.
- (iii) Modelling of soil systems with conventional finite element and super element to reduce the computational time and effort without sacrificing the accuracy.
- (iv) Examination of the effect of different types of soil (soft to stiff) on the overall interactive behaviour of the shear wall foundation soil system.

The formulation of the Modified Optimal Triangular (MOPT) element and generation of the super element are presented in subsequent sections.

## 2. Formulation of optimal membrane elements

Felippa and co-workers are the key contributors in the development of elements with drilling degrees of freedom (Felippa 1996, 2003, Felippa and Alexander 1992, Felippa and Militello 1992) They have developed elements of this sort that are appropriate for the two dimensional representation of shear wall structures.

In this study, the Natural Deviatoric Strain (ANDES) formulation and the Natural Strain (ANS) method is applied (Park and Stanley 1986). ANDES is a variant of ANS that exploits the fundamental decomposition of the stiffness as follows

$$K_R = (K_b + \alpha K_h) V \quad (1)$$

Here  $K_b$  is the basic stiffness, which satisfies consistency and  $K_h$  is the higher order stiffness which deals with stability (rank sufficiency) and accuracy and  $\alpha$  is scaling coefficient with positive magnitude. The basic stiffness matrix  $K_b$  is constructed by the standard procedure, i.e. for the constant strain triangular (CST) element. An explicit form of the basic stiffness for the linear strain triangle (LST) was obtained in 1984 and published the following year. It can be expressed as  $K_b = V^{-1} L E L^T$ , where  $V = Ah$  is the element volume,  $A$  the area,  $h$  the thickness, and  $L$  is a  $3 \times 9$  matrix that contains a free parameter  $\alpha_b$  (Bergan 1985)

$$L = \frac{1}{2} h \begin{bmatrix} y_{23} & 0 & x_{23} \\ 0 & x_{23} & y_{23} \\ \frac{1}{6} \alpha_b y_{23} (y_{13} - y_{21}) & \frac{1}{6} \alpha_b x_{32} (x_{31} - x_{12}) & \frac{1}{3} \alpha_b (x_{31} y_{13} - x_{12} y_{21}) \\ y_{31} & 0 & x_{13} \\ 0 & x_{13} & y_{31} \\ \frac{1}{6} \alpha_b y_{31} (y_{21} - y_{32}) & \frac{1}{6} \alpha_b x_{13} (x_{12} - x_{23}) & \frac{1}{3} \alpha_b (x_{12} y_{21} - x_{23} y_{32}) \\ y_{12} & 0 & x_{21} \\ 0 & x_{21} & y_{12} \\ \frac{1}{6} \alpha_b y_{12} (y_{32} - y_{13}) & \frac{1}{6} \alpha_b x_{21} (x_{23} - x_{31}) & \frac{1}{3} \alpha_b (x_{23} y_{32} - x_{31} y_{13}) \end{bmatrix} \quad (2)$$

In the free formulation (FF) this is called a force-lumping matrix, If  $\alpha_b = 0$  the basic stiffness reduces to the total stiffness matrix of the Constant Strain Triangle (CST) element. For this case, the rows and columns associated with the drilling rotations vanish.

The mean portion of the strains is left to be determined from the constant stress assumptions used to develop  $K_h$ . The main advantage of ANDES over ANS is that elements constructed with the former technique are guaranteed to pass the individual element test (Bergan 1985, Park and Stanley 1986). In the derivation of the higher order stiffness by ANDES, the natural strains play a key role. The ANDES form of the higher order stiffness matrix  $K_h$  has been derived by some researchers as (Felippa and Alexander 1992, Paknahad, Noorzaei *et al.* 2007)

$$K_h = C_{fac} T_{\theta u}^T K_{\theta} T_{\theta u} \quad (3)$$

In which  $K_{\theta}$  is the higher order stiffness in terms of hierarchical rotations and depends on nine free dimensionless parameters  $\beta_1$  through  $\beta_9$ , as will be explained below. First, the matrix  $Q_i$  that relates the natural strains  $i$  at corner  $i$  to the deviatoric corner curvatures  $\theta$  of the triangle can be given as follows

$$Q_1 = \frac{2A}{3} \begin{bmatrix} \beta_1 & \beta_2 & \beta_3 \\ l_{21}^2 & l_{21}^2 & l_{21}^2 \\ \beta_4 & \beta_5 & \beta_6 \\ l_{32}^2 & l_{32}^2 & l_{32}^2 \\ \beta_7 & \beta_8 & \beta_9 \\ l_{13}^2 & l_{13}^2 & l_{13}^2 \end{bmatrix} \quad (4a)$$

$$Q_2 = \frac{2A}{3} \begin{bmatrix} \beta_9 & \beta_7 & \beta_8 \\ l_{21}^2 & l_{21}^2 & l_{21}^2 \\ \beta_3 & \beta_1 & \beta_2 \\ l_{32}^2 & l_{32}^2 & l_{32}^2 \\ \beta_6 & \beta_4 & \beta_5 \\ l_{13}^2 & l_{13}^2 & l_{13}^2 \end{bmatrix} \quad (4b)$$

$$Q_3 = \frac{2A}{3} \begin{bmatrix} \beta_5 & \beta_6 & \beta_4 \\ l_{21}^2 & l_{21}^2 & l_{21}^2 \\ \beta_8 & \beta_9 & \beta_7 \\ l_{32}^2 & l_{32}^2 & l_{32}^2 \\ \beta_2 & \beta_3 & \beta_1 \\ l_{13}^2 & l_{13}^2 & l_{13}^2 \end{bmatrix} \quad (4c)$$

of which the values at the midpoints are as follows

$$Q_4 = \frac{1}{2}(Q_1 + Q_2) \quad (5a)$$

Table 1 Dimensionless parameter of OPT element

$\alpha_b$	$\beta_0$	$\beta_1$	$\beta_2$	$\beta_3$	$\beta_4$	$\beta_5$	$\beta_6$	$\beta_7$	$\beta_8$	$\beta_9$
3/2	1/2	1	2	1	0	1	-1	-1	-1	-2

$$Q_5 = \frac{1}{2}(Q_2 + Q_3) \quad (5b)$$

$$Q_6 = \frac{1}{2}(Q_3 + Q_1) \quad (5c)$$

Then the matrix  $K_\theta$  can be related to above quantities as

$$K_\theta = h(Q_4^T E_{nat} Q_4 + Q_5^T E_{nat} Q_5 + Q_6^T E_{nat} Q_6) \quad (6)$$

In which  $E_{nat}$  is the natural stress-strain matrix. The stiffness matrix  $K_h$  can be given as follows

$$K_h = \frac{3}{4} \beta_0 T_{\theta u}^T K_\theta T_{\theta u} \quad (7)$$

Where  $\beta_0$  is an overall scaling coefficient. Finally  $K_R$ , which is the fundamental decomposition of stiffness, see Eq. (1), initially constructed by combining basic stiffness ( $K_b$ ) and the higher order stiffness ( $K_h$ ), assumes a template form with 11 free parameters (Felippa 1996, 2003), i.e.  $\alpha_b, \beta_0, \beta_1, \dots, \beta_9$ .

$$K_R(\alpha_b, \beta_0, \beta_1, \dots, \beta_9) = V^{-1} L E L^T + \frac{3}{4} \beta T_{\theta u}^T K_\theta T_{\theta u} \quad (8)$$

In which  $V$  is the element volume, i.e.  $V = Ah$ ,  $L$  is the free-lumping matrix and  $T_{\theta u}$  stands for the transformation matrix. The free dimensionless parameters  $\alpha_b, \beta_0$  through  $\beta_9$  are determined from a higher order patch test that tunes up the higher order stiffness of the triangular elements. Their values are listed in Table 1.

### 3. A fast calculation of higher order stiffness matrix

In this study, an alternative formulation of the above element is presented, which turns out to be more efficient than the optimal element proposed by Felippa (2003). Let us assume the LL matrix as

$$LL = \begin{bmatrix} l_{21}^2 & 0 & 0 \\ 0 & l_{32}^2 & 0 \\ 0 & 0 & l_{13}^2 \end{bmatrix} \quad (9)$$

With this matrix, we can rewrite the  $Q_i, T_e$  and  $E_{nat}^*$  matrices as

$$Q_i = LL^{-1} Q_i^* \quad (10a)$$

$$T_e = T_e^* LL \quad (10b)$$

$$E_{nat}^* = T_e^* E T_e^* \quad (10c)$$

$Q_i^*$  and  $T_e^*$  are as follows

$$Q_i^* = \frac{2A}{3} \begin{bmatrix} \beta_1 & \beta_2 & \beta_3 \\ \beta_4 & \beta_5 & \beta_6 \\ \beta_7 & \beta_8 & \beta_9 \end{bmatrix} \quad Q_2^* = \frac{2A}{3} \begin{bmatrix} \beta_9 & \beta_7 & \beta_8 \\ \beta_3 & \beta_1 & \beta_2 \\ \beta_6 & \beta_4 & \beta_5 \end{bmatrix} \quad Q_3^* = \frac{2A}{3} \begin{bmatrix} \beta_5 & \beta_6 & \beta_4 \\ \beta_8 & \beta_9 & \beta_7 \\ \beta_2 & \beta_3 & \beta_1 \end{bmatrix}$$

$$T_e^* = \frac{1}{4A^2} \begin{bmatrix} y_{23}y_{13} & y_{31}y_{21} & y_{12}y_{32} \\ x_{23}x_{13} & x_{31}x_{21} & x_{12}x_{32} \\ y_{23}x_{31} + x_{32}y_{13} & y_{31}x_{12} + x_{13}y_{21} & y_{12}x_{23} + x_{21}y_{32} \end{bmatrix}$$

In addition,

$$Q_4^* = LL^{-1}Q_4 \quad Q_5^* = LL^{-1}Q_5 \quad Q_6^* = LL^{-1}Q_6$$

Substituting the new form of  $T_e$  and  $Q_i$  in the high order stiffness formulation  $K_\theta$ , Eq. (6), and expanding, one has

$$K_\theta = h((LL^{-1}Q_4^*)^T (T_e^*LL)^T E(T_e^*LL)(LL^{-1}Q_4^*) + (LL^{-1}Q_5^*)^T (T_e^*LL)^T E(T_e^*LL)(LL^{-1}Q_5^*) + (LL^{-1}Q_6^*)^T (T_e^*LL)^T E(T_e^*LL)(LL^{-1}Q_6^*)) \quad (11)$$

After simplification

$$K_\theta = h(Q_4^{*T} E_{nat}^* Q_4^* + Q_5^{*T} E_{nat}^* Q_5^* + Q_6^{*T} E_{nat}^* Q_6^*) \quad (12)$$

Hence the formulation of the matrix  $K_h$  with new notation is more efficient in terms of computational time and effort compared with that of Felippa (2003). The same formulation has been adopted for the calculation of stresses.

#### 4. Generation of super element in shear wall system

The stiffness matrix of each super element is calculated independently and the super element is subsequently joined to other elements in the overall analysis. Kim and Lee (2003) presented the super element for the analysis of shear walls with openings, (Paknahad, Noorzaei *et al.* 2009).

Fig. 1 briefly shows the computational strategy used in the present study to generate the super element, including the assembly and final configuration of a shear wall building. The procedure enables us to systematically reduce the number of assembled equations on different substructure levels. The process of the super element generation is as follows:

- Selecting the type of super element based on geometrical configuration of the considered structural system and fixing the position of super elements,
- Generating the finite element mesh utilizing the eight node isoparametric elements,
- Evaluating the stiffness matrix for each element,
- Applying the condensation technique Eq. (13) and extracting the super element stiffness matrix,
- Writing down the stiffness matrix of super elements on an auxiliary device and prepare for assembly of stiffness matrix (Paknahad 2008, Paknahad, Noorzaei *et al.* 2009).

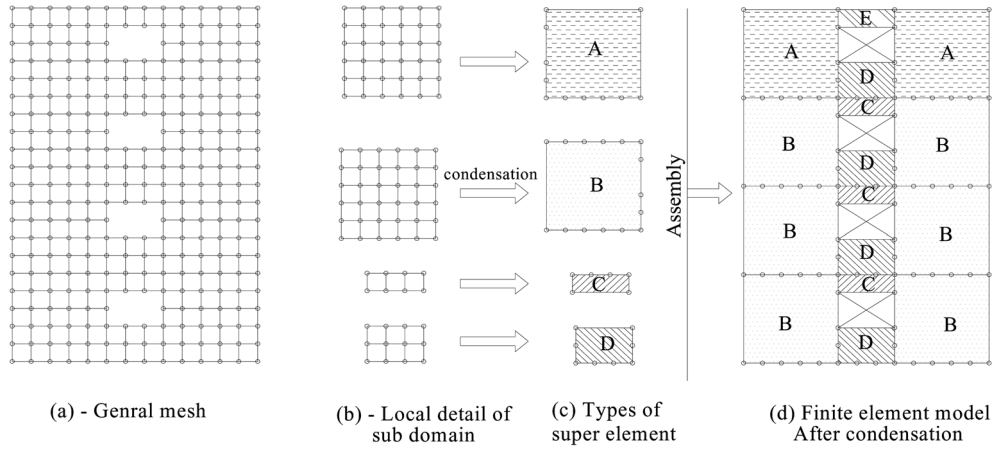


Fig. 1 Implementation of super elements

Table 2 Column dimensions

	Grid A		Grid B		Grid C		Grade	Ec (N/mm <sup>2</sup> )
	Depth (mm)	Width (mm)	Depth (mm)	Width (mm)	Depth (mm)	Width (mm)		
20 <sup>th</sup> to Roof	600	600	675	600	675	600	C40	28
15 <sup>th</sup> to 20 <sup>th</sup>	600	600	900	600	825	600	C40	28
10 <sup>th</sup> to 15 <sup>th</sup>	675	600	1125	600	900	600	C40	28
5 <sup>th</sup> to 10 <sup>th</sup>	825	600	1425	600	1050	600	C40	28
G to 5 <sup>th</sup>	1050	600	1650	600	1275	600	C40	28
LG3 to G	1200	600	1800	600	1500	600	C45	29

$$(K_{rr} - K_{rc}K_{cc}^{-1}K_{cr})U_r = R_r - K_{rc}K_{cc}^{-1}R_c \quad (13)$$

The  $K_{rr}$ ,  $K_{rc}$  and  $K_{cc}$  are stiffness matrix and  $R_r$  and  $R_c$  are external load vector corresponded to displacements  $U_r$  and  $U_c$ , where subscripts “r” and “c” indicate the retained and condensed degree of freedom respectively.

## 5. Analysis of 28 story building system

Let us consider a 28<sup>th</sup> storey, three bay plane frame, supported by piles of unequal lengths with sockets embedded into the rock at a depth of 2 m. Pile A ends at a depth of 19 m, pile B at a depth of 15 m and pile C at a depth of 11m. This frame structure-piles system is supported by four layers of soil and a rock layer, with their nonlinear stress-strain characteristics taken into account. The material properties, geometry and loadings of the superstructure are shown in Tables 2, 3 and Fig. 2, respectively. The vertical and lateral loadings acting on the building are presented in Fig. 2.

The tangent modulus,  $E_i$  of the top to the most bottom soil layer is 52.49, 122.51, 187.25 and 205.37 kg/cm<sup>2</sup>, respectively. The Finite Element Mesh configuration of the system is shown in Fig. 3. The soil boundary between the soil and rock is represented in the figure by a line passing

Table 3 Beam dimensions

	Grid A to Grid B		Grid B to Grid C		Grade
	Depth (mm)	Width (mm)	Depth (mm)	Width (mm)	
Roof	600	600	600	600	C30
11 <sup>th</sup> to 24 <sup>th</sup>	600	375	600	375	C30
1 <sup>st</sup> to 10 <sup>th</sup>	600	300	600	300	C30
LG2 to G	600	300	600	300	C35
LG3	600	450	600	450	C35

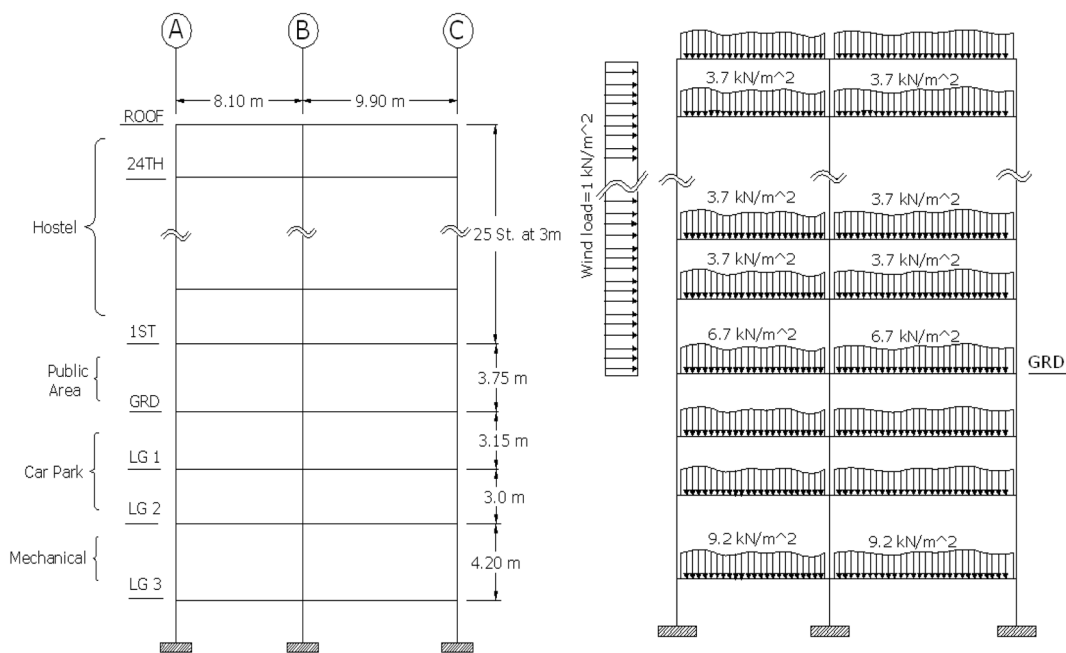


Fig. 2 Frame dimensions

through the soil strata. The symbol B denotes the width of the superstructure. The upper layer consists of soil and the lower layer consists of rock. The detailed configuration of the superstructure is shown in Fig. 2.

The following analyses were performed on the above structure:

- Non-Interactive Analysis (NIA).
- Linear Interactive Analysis (LINA).

### 5.1 Results and discussion

The displacements in various columns and the maximum displacements of the beams of the frame obtained by the two methods, namely, the Non Interactive Analysis (NIA) and Linear Interactive Analysis (LIA), were listed in Table 5. As can be seen, the displacement due to the interactive analysis is higher compared with the non interactive analysis. This is due to the fact that NIA ignores the effect of soil compressibility, as the base is assumed to be fixed to the ground, and vice

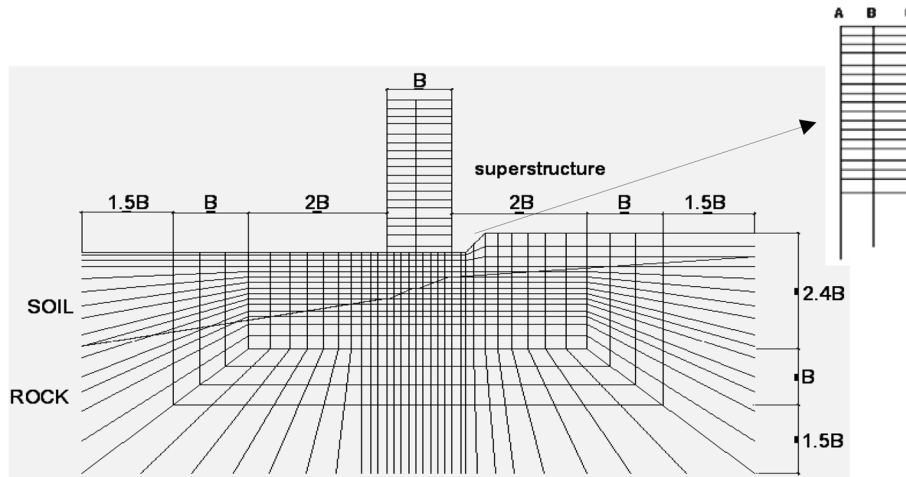


Fig. 3 Finite element mesh

Table 4 Maximum displacements of beams and columns by the two analyses

		Max. Beam Displ. (mm)		Max. Column Displ. (mm)		
		–		A	B	C
Analysis	NIA	12.241		64.447	64.525	64.576
	LIA	14.926		83.233	83.20	83.094

Table 5 Soil properties for different types of soils (Selvadurai 1979)

No	Soil types	$E$ (kN /m <sup>2</sup> )	$\nu$
1	Sandy clay	35000	0.32
2	Gravely sand	57600	0.30
3	Dense gravely sand	95000	0.25

versa for the interactive analysis. Moreover, the maximum lateral displacement of LIA is approximately 1.3 to 1.4 times higher than that of NIA respectively. This is due to the fact that the LIA considers the settlement of the soil.

The variation of lateral displacement of the piles by LIA is plotted in Fig. 4. It is clear that the pattern of the displacement for each pile is rather similar, whereby the displacement diminishes as the depth increase. This is due to the inclined strata of bedrock and unequal lengths of the piles. The trend of displacement decreases nearly to zero for the pile end with socket embedded in the bedrock. Since the rock is a very stiff material, the displacement in the rock is nearly zero. In addition, the displacement of each pile becomes zero at different depths.

Fig. 5 shows the variation of lateral displacement along pile and soil depth obtained by different analyses, from which it can be seen that the difference in displacement between the pile and soil (rock) is approximately in the range of 6 to 8 mm.

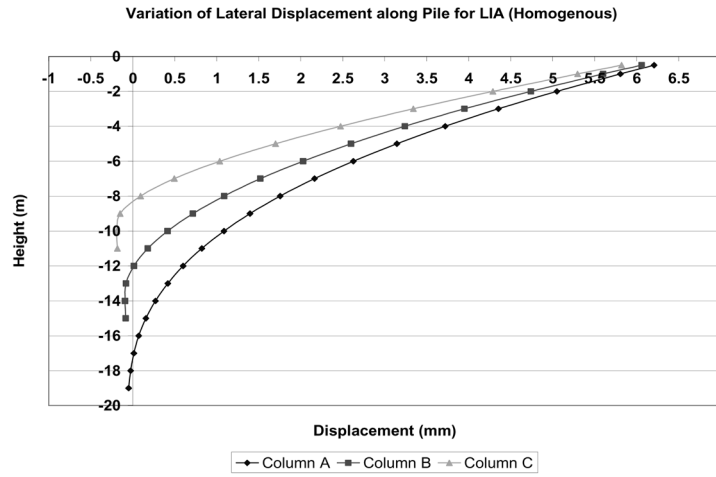


Fig. 4 Variation of lateral displacement of piles (LIA)

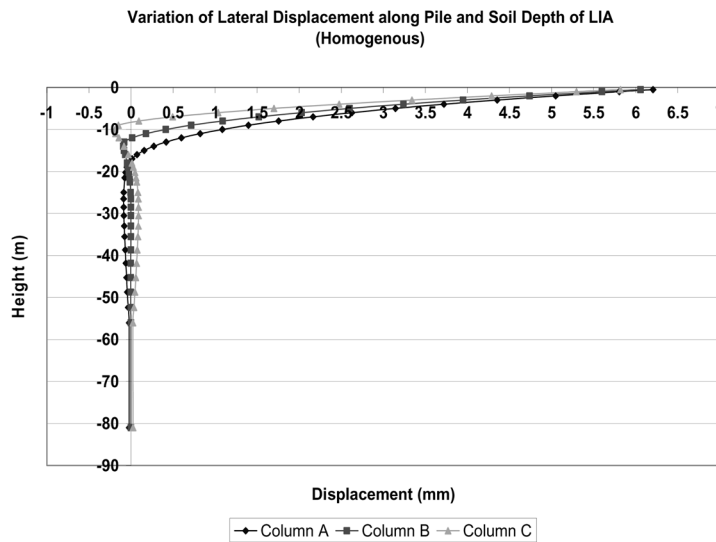


Fig. 5 Variation of horizontal displacement along pile and soil depth (LIA)

### 6. Analysis of shear wall buildings with openings

The application of the proposed finite element model for the shear wall foundation soil system is demonstrated in the analysis of an 8-story shear wall building. Fig. 6 shows the material and geometry of the shear wall considered, which has a height of 32 m, width of 10 m and thickness of 0.4 m. The material property and locations of the openings along the height are also shown in this figure. In the non-interactive analysis, two finite element models are used:

Model I: Constructed by eight-node conventional isoparametric element as shown in Fig. 6(b).

Model II: Constructed by two types of super element respectively for the main shear wall area with 20 nodes and the connection beam with 6 nodes in Fig. 6(c).

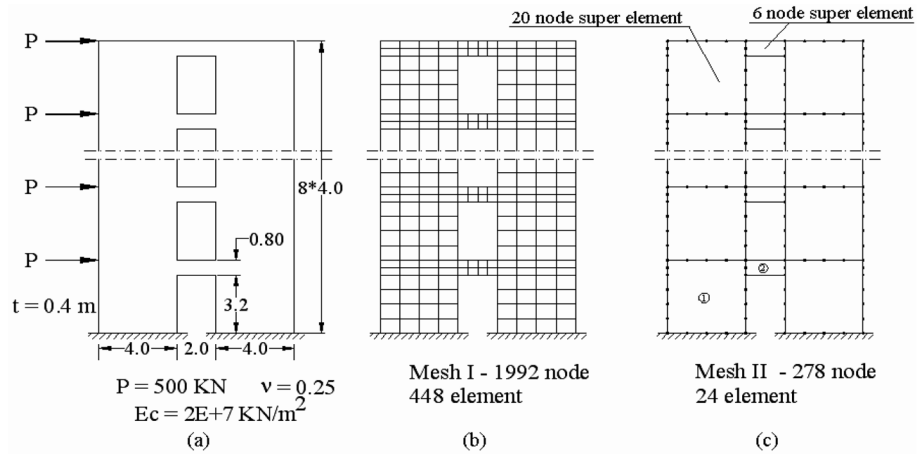


Fig. 6 Geometry, material and mesh generation of shear wall with openings

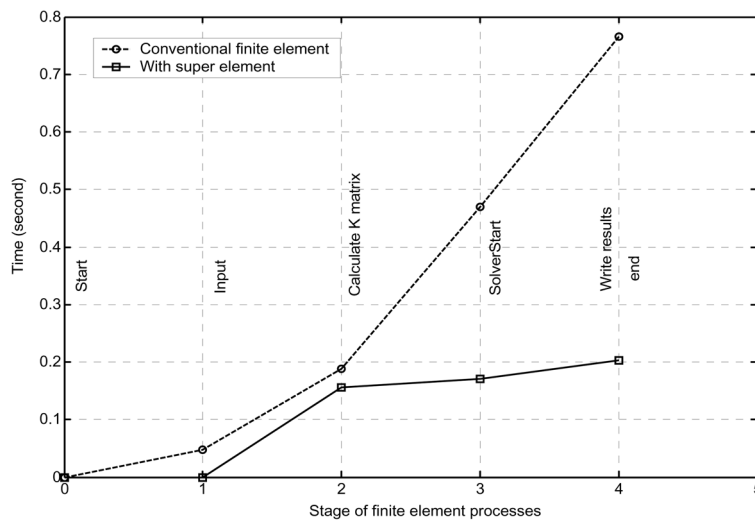


Fig. 7 Computation time versus different stages of analysis

### 6.1 Discussion and comparison of the results

The computational time versus the different stages of finite element operation corresponding to both structural models are presented in Fig. 7. It is clear from this plot that there is a considerable reduction in the computational time in using the super element model as compared with the conventional eight-node finite element model, the latter has a computation time of 350 % higher. This is an indication of the efficiency of using the super element.

The variation of horizontal displacement along the height of the shear wall is shown in Fig. 8. As depicted in this figure, the displacements of all the retained nodes of the super element model are coincident with those obtained by the conventional finite element model (model I).

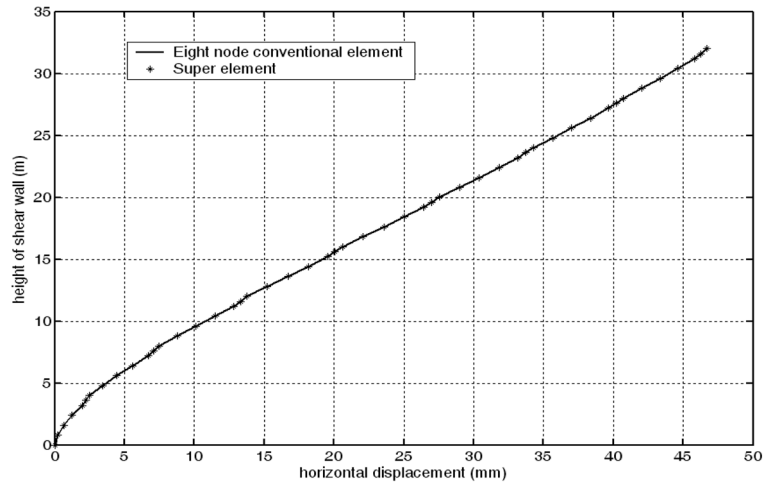


Fig. 8 Horizontal displacement of shear wall

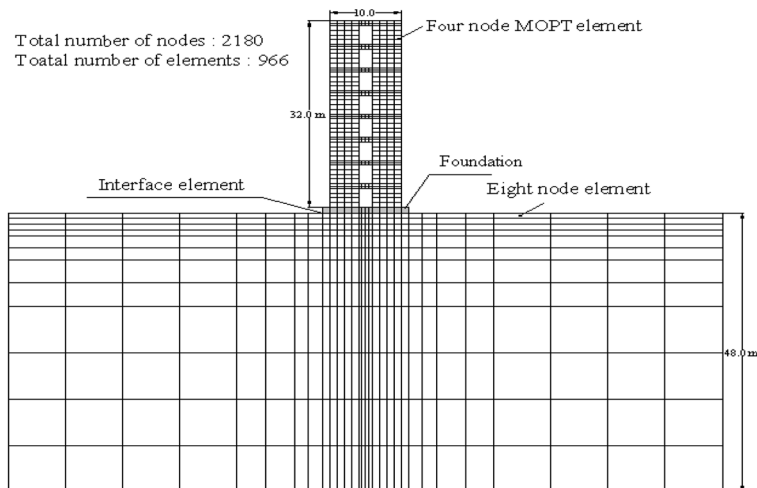


Fig. 9 Finite element mesh of shear wall foundation with soil media (MOPT and conventional elements)

## 7. Linear interactive analysis via MOPT and conventional finite elements

The finite element mesh used in modeling has been shown in Fig. 9. The modified optimal triangular element (MOPT) was used to model the super structure and foundation, while the eight-node isoparametric element was employed to discretise the soil media. The effect of stiffness of the soil was investigated by using three types of soil, of which the material properties are listed in Table 7.

### 7.1 Discussion of results

Figs. 10 (a) and (b), respectively, shows the horizontal and vertical displacements of the shear wall along its height. From these figures, the effect of different stiffnesses of the soil on the

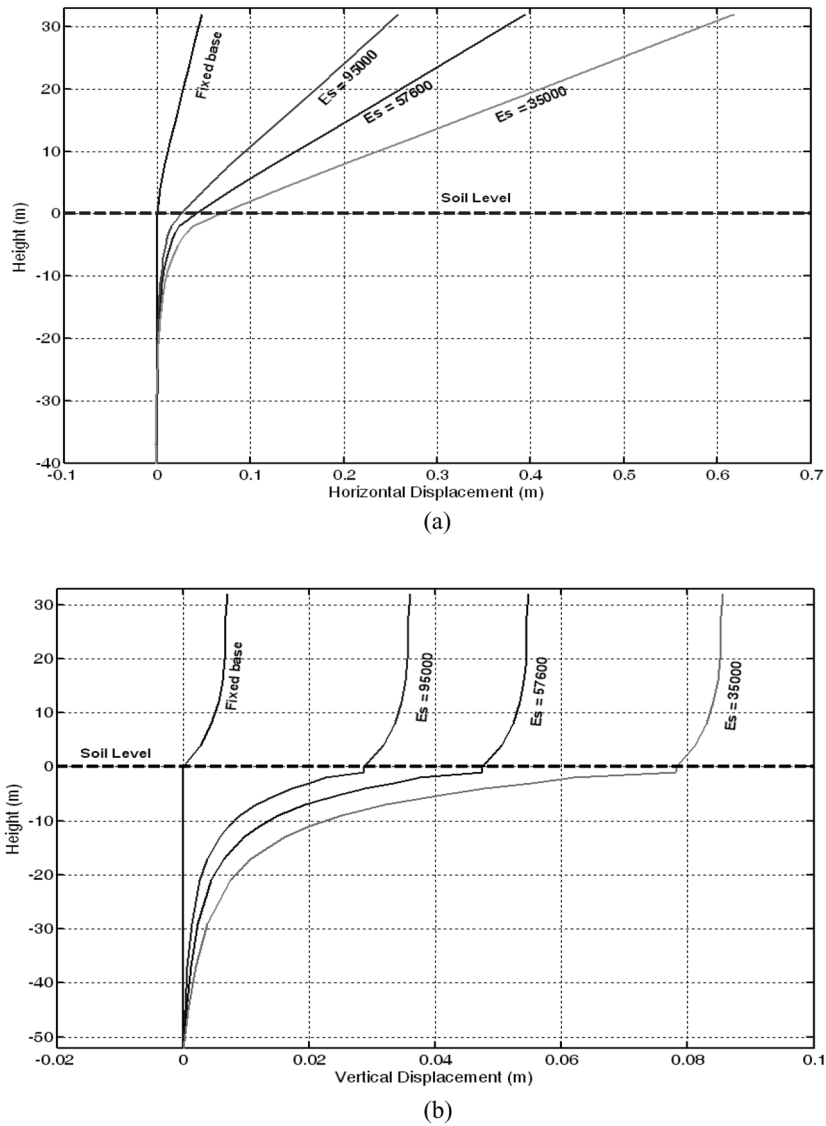


Fig. 10 Displacements of shear wall – foundation – soil media: (a) Horizontal, (b) Vertical

response of the shear wall building can be clearly observed. For the soil with Young’s modulus of elasticity as  $E_s = 35000, 57600$  and  $95000 \text{ kN/m}^2$ , the top horizontal displacement was calculated to be  $0.607, 0.387$  and  $0.254 \text{ m}$ , respectively. Clearly, the maximum displacements occur at the top and the minimum displacements at the base of the soil media. Also, the effect of soft soil on both the vertical and horizontal displacements of the shear wall structure can be appreciated.

The normal stress across the width of shear wall at an elevation of  $48.281 \text{ m}$  below the superstructure obtained by the interactive analysis is compared with that of the non interactive analysis in Fig. 11. It can be seen that the support condition leads to a distribution of stress in the shear wall. Furthermore, this figure indicates high concentration of stresses at the corners of wall originated by flexibility of the soil, resulting in stress redistribution in the shear wall.

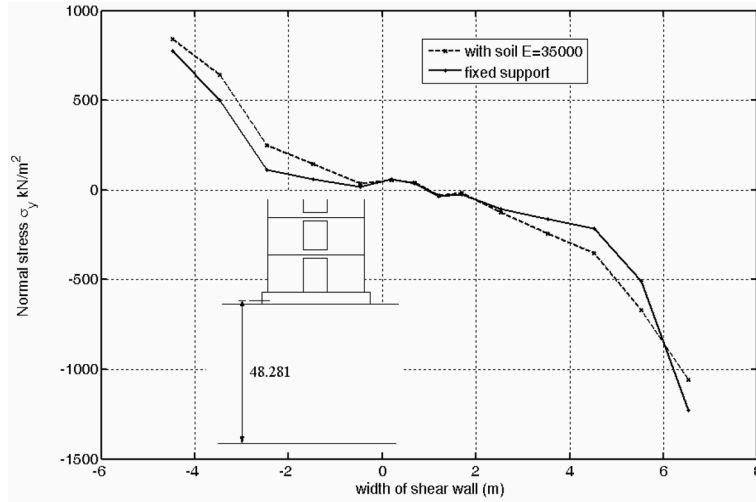


Fig. 11 Comparison of normal stress along the width of shear wall at elevation 48.281

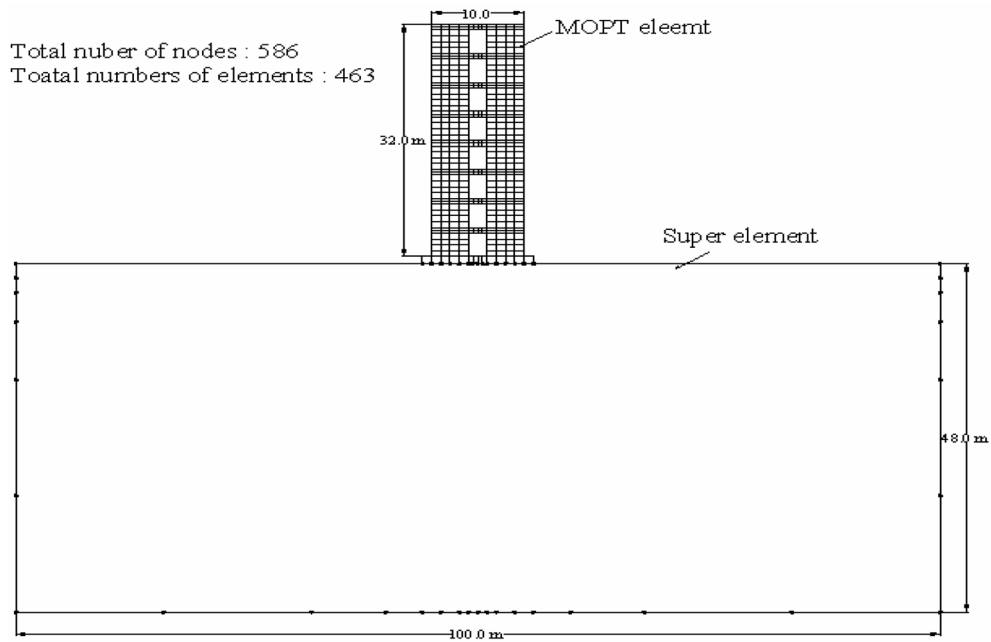
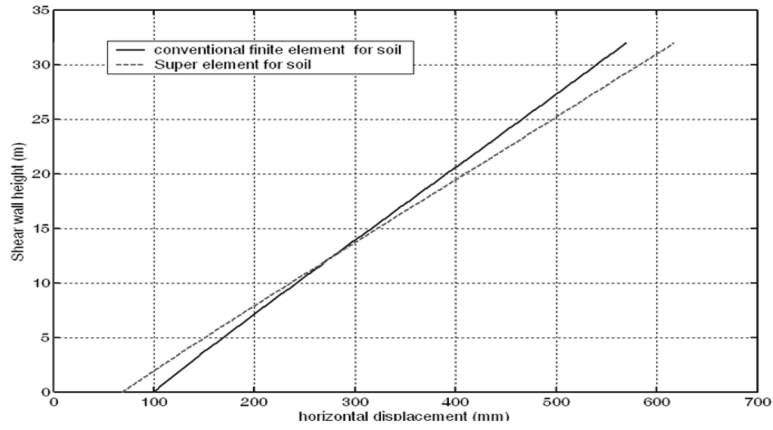


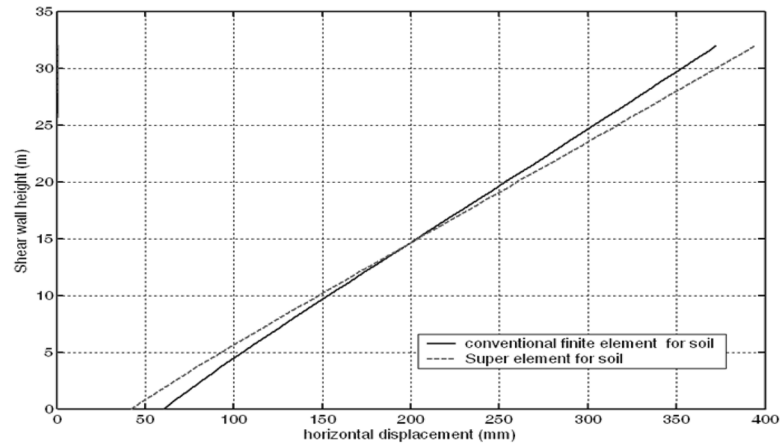
Fig. 12 Finite element discretisation of shear wall-foundation-soil media using MOPT and super element

### 8. Linear interactive analysis with MOPT and super element

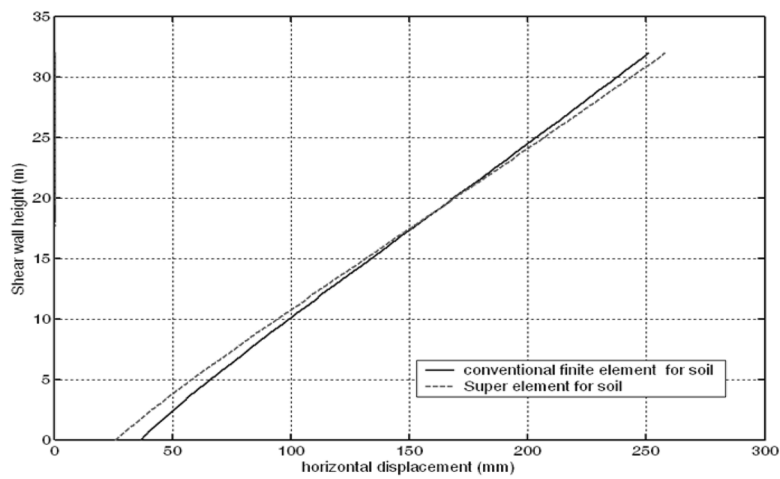
As a further demonstration of the application of the super element, an attempt has been made to represent the super structure by MOPT and the soil media by the super element. Fig. 12 shows the finite element mesh used in modeling of the superstructure, foundation and soil system. In this mesh, the MOPT element has been used to represent the superstructure and the foundation, and a



(a)



(b)



(c)

Fig. 13 Horizontal displacements of shear wall-soil media: (a)  $E = 35000$ , (b)  $E = 57600$ , (c)  $E = 95000$  kN/m<sup>2</sup>

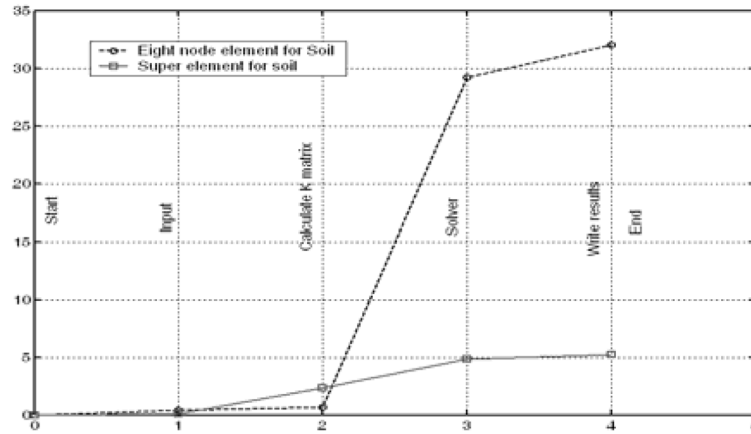


Fig. 14 Computational time versus different stages of analysis

super element with 44 nodes has been generated for the soil media. In the generation of the super element, initially the soil was discretised by eight-node isoparametric element and then the computational algorithm was activated to generate the super element. Effort has been made to always maintain compatibility at the contact nodes between the foundation and soil media.

### 8.1 Discussion of results

An attempt has been made to compare the present results with those obtained by previous finite element model. The variation of lateral displacements along the height of the shear wall for three types of soil is illustrated in Fig. 13. It is clear from these plots that the maximum displacement of 250 mm occurs at the top and the minimum displacement of 37.2 mm at the foundation level. However the relative displacement of 100.2% at the top and 78% at the bottom predicted by both idealizations are almost the same. These figures show that the super element can provide a good estimate of the displacement for the shear wall structure. Similar trend was observed for different types of soil.

Fig. 14 shows the computational time taken at different steps for the analysis of the shear wall building foundation soil system. This plot clearly illustrates the efficiency of the super element in the analysis of shear wall - foundation -soil media. The computation time needed for analysis with the super element case is around 6 times less than that of the conventional finite element method.

## 9. Conclusions

The major conclusions drawn from the element formulation and numerical analyses presented in this paper are as follows:

- Optimal triangle element was formulated and its computational efficiency was found in representation of shear wall system.
- The finite element idealization using the super element – finite element model is very encouraging when the displacement and stress analysis of the super structure – foundation – soil

media is of primary concern.

- The effect of interaction between the soil and shear wall is important and cannot be neglected to ensure the accuracy of the result. The interaction analysis shows remarkable difference in the displacements and stress distribution of the shear wall.
- Different types of soil have significant effect on the displacement and stress response of the shear wall. There is a marked increase in the maximum deflection, say, 25%, of the shear wall–foundation–soil due to inclusion of soil nonlinearity.
- Accurate results can be obtained by using plane strain soil element along with an infinite element to account for the semi-infinite extent of the soil domain.
- As for interactive behavior, it has been realized that the total settlement obtained from the linear interactive analysis is about 1.3 to 1.4 times that of the non-interactive analysis.

## Acknowledgments

The financial support for this research is provided by King Saud University, Saudi Arabia under grant number of 67001. This support is gratefully acknowledged and appreciated.

## References

- Badie, S. and Salmon, D. (1996), “A quadratic order elastic foundation finite element”, *Comput. Struct.*, **58**(3), 435-443.
- Badie, S. and Salmon, D. (1997), “Three-noded curved isoparametric soil interface element”, *Comput. Struct.*, **65**(2), 205-212.
- Badie, S., Salmon, D. and Beshara, A. (1997), “Analysis of shear wall structures on elastic foundations”, *Comput. Struct.*, **65**(2), 213-224.
- Bergan, C. (1985), “A triangular membrane element with rotational degrees of freedom”, *Comput. Method. Appl. M.*, **50**(1), 25-69.
- Boroschek, R. and Yáñez, F. (2000), “Experimental verification of basic analytical assumptions used in the analysis of structural wall buildings”, *Eng. Struct.*, **22**(6), 657-669.
- Chore, H., Ingle, R. and Sawant, V. (2009), “Building frame-pile foundation-soil interactive analysis”, *Interact. Multiscale Mech.*, **2**(4), 397-411.
- Chore, H., Ingle, R. and Sawant, V. (2010a), “Building frame-pile foundation-soil interaction analysis: a parametric study”, *Interact. Multiscale Mech.*, **3**(1), 55-79.
- Chore, H., Ingle, R. and Sawant, V. (2010b), “Parametric study of pile groups subjected to lateral load”, *Struct. Eng. Mech.*, **36**(2), 243-246.
- Dutta, S. and Roy, R. (2002), “A critical review on idealization and modeling for interaction among soil-foundation-structure system”, *Comput. Struct.*, **80**(20-21), 1579-1594.
- Felippa, C. and Alexander, S. (1992), “Membrane triangles with corner drilling freedoms - III. Implementation and performance evaluation”, *Finite Elem. Anal. Des.*, **12**(3-4), 203-239.
- Felippa, C. and Militello, C. (1992), “Membrane triangles with corner drilling freedoms - II. The ANDES element”, *Finite Elem. Anal. Des.*, **12**(3-4), 189-201.
- Felippa, C. (1996), “Refined finite element analysis of linear and nonlinear two-dimensional structures”, *Structures and Materials Research*, Dept. of Civil Engineering, Univ. of Calif., Berkeley, Report, 66-22.
- Felippa, C. (2003), “A study of optimal membrane triangles with drilling freedoms”, *Comput. Method. Appl. M.*, **192**(16-18), 2125-2168.
- Kim, H. and Lee, D. (2003), “Analysis of shear wall with openings using super elements”, *Eng. Struct.*, **25**(8), 981-991.

- Nadjai, A. and Johnson, D. (1998), "Elastic and elasto-plastic analysis of planar coupled shear walls with flexible bases", *Comput. Struct.*, **68**(1-3), 213-229.
- Noorzaei, J., Alkarni, A., Jaafar, M.S. and Dalili, M. (2010), "Modelling of soil structure interaction in framed and shear wall structures", *The First International Conference on Advances in Interaction and Multiscale Mechanics*, Jeju, Korea.
- Paknahad, M., Noorzaei, J., Jaafar, M. and Thanoon, W. (2007), "Analysis of shear wall structure using optimal membrane triangle element", *Finite Elem. Anal. Des.*, **43**(11-12), 861-869.
- Paknahad, M. (2008), *Development of finite element codes for shear wall analysis*, Ph.D Thesis, Civil Engineering, Universiti Putra Malaysia.
- Paknahad, M., Noorzaei, J., Jaafar, M. S. and Thanoon, W.A.M. (2009), "Nonlinear analysis of shear wall system with Super element", *Struct. Eng.*, **36**(5), 319-326.
- Pandey, A.K., Kumar, G. and Shamra, S.P. (1994), "An interactive approach for the soil-structure interaction in tall buildings", *Eng. Fract. Mech.*, **41**(2), 169-176.
- Park, K. and Stanley, G. (1986), "A curved C° shell element based on assumed natural-coordinate strains", *J. Appl. Mech.*, **53**, 278-290.
- Viladkar, M., Godbole, P. and Noorzaei, J. (1991), "Soil-structure interaction in plane frames using coupled finite-infinite elements", *Comput. Struct.*, **39**(5), 535-546.
- Viladkar, M., Godbole, P. and Noorzaei, J. (1992a), "Space frame-raft-soil interaction including effect of slab stiffness", *Comput. Struct.*, **43**(1), 93-106.
- Viladkar, M., Sharma, R. and Ranjan, G. (1992b), "Visco-elastic finite element formulation for isolated foundations on clays", *Comput. Struct.*, **43**(2), 313-324.
- Viladkar, M., Godbole, P. and Noorzaei, J. (1994a), "Modelling of interface for soil-structure interaction studies", *Comput. Struct.*, **52**(4), 765-779.
- Viladkar, M., Noorzaei, J. and Godbole, P. (1994b), "Behaviour of infinite elements in an elasto-plastic domain", *Comput. Struct.*, **51**(4), 337-342.